

seen from the figures, Eq. (15) gives a better approximation than (14) for small μt , but is not as good for larger μt .

Finally, we apply this approximation technique to the example of Section 2. Suppose the following "static" information about the network of Fig. 1 is known: $\rho_1 = .9$, $\rho_2 = .5$, $\mu_1 = 6$, $\mu_2 = 6$. $K = 20$ for both buffers,

A JSQ decision is to be made at time $t = 4$ to route a packet via either node 1 or 2 based on the most recent queue length information:

$$N_1(0) = 0$$

$$N_2(1) = 10.$$

Using the first order approximation (14) we find from Fig. 3a and c

$$\bar{N}_1(4) \approx 3.9$$

$$\bar{N}_2(4) \approx 2.5$$

so that the decision would be to send the packet to node 2. (The exact values of \bar{N}_1 and \bar{N}_2 would yield the same decision.)

5. CONCLUSIONS

By using a finite Markov chain model, an exact closed form expression for the transient behavior of an $M/M/1$ queue with finite storage has been derived. It has been shown that this expression is in a form which lends itself to simple approximations for the dynamic behavior of mean queue length. To a certain extent, the results obtained here are analogous to those obtained using diffusion approximations. Specifically, the representation (8) corresponds to the eigenfunction expansion of the solution of the diffusion equation in Ref. 10. However, diffusion approximations are only valid for $\rho \approx 1$ while our results are not limited to this case.

We have also illustrated how the approximations can be used in certain adaptive routing schemes. The fact that the simple approximations described above have been obtained for an isolated queue suggests that similar approaches may be fruitful for networks of queues. If a reasonably simple dynamic model for a queueing network were derived using these approaches, it would be of considerable value in the design and analysis of various network control algorithms.

ACKNOWLEDGMENT

The author wishes to thank Prof. D. R. Smith of Columbia University for calling his attention to Ref. 8.

REFERENCES

- [1] A. Livne, "Dynamic Routing in Computer Communication Networks," Doctoral Dissertation, Dept. of Electrical Engineering and Electrophysics, PINY, 1977
- [2] C. W. Brown and M. Schwartz, "Adaptive Routing in Centralized Computer Communication Networks," *Proc. ICC*, San Francisco, June 1975
- [3] J. M. McQuillan and D. C. Walden, "The ARPA Network Design Decisions," *Computer Networks*, 1 243-289 (1977)
- [4] T. S. Yum and M. Schwartz, "Analysis of a Class of Locally-

Adaptive Routing Rules in Computer Communication Networks," submitted for publication.

- [5] T. S. Yum and M. Schwartz, "The Join-Biased-Queue (JBQ) Rule and its Application to Routing in Computer Communication Networks," submitted for publication.
- [6] G. Foschini and J. Salz, "A Basic Dynamic Routing Problem and Diffusion," *IEEE Trans. Commun.*, COM-26, 320-327 (1978)
- [7] D. R. Cox and W. L. Smith, *Queues*, Chapman and Hall, London, 1961
- [8] J. Keilson, "Markov Chain Models-Rarity and Exponentiality," Report No. CSS 74-01, Center for System Science, University of Rochester, Rochester, N.Y., Sept. 1974
- [9] F. B. Hildebrand, *Finite Difference Equations and Simulations*, Prentice-Hall, Englewood Cliffs, N.J., 1968
- [10] H. Kobayashi, "Application of the Diffusion Approximation to Queuing Networks II: Nonequilibrium distributions and Applications to Computer Modeling," *J. ACM* 21, 459-469 (1974)

Image Compression Using Block Truncation Coding

EDWARD J. DELP, STUDENT MEMBER, IEEE, AND
O. ROBERT MITCHELL, MEMBER, IEEE

Abstract—A new technique for image compression called Block Truncation Coding (BTC) is presented and compared with transform and other techniques. The BTC algorithm uses a two-level (one-bit) nonparametric quantizer that adapts to local properties of the image. The quantizer that shows great promise is one which preserves the local sample moments. This quantizer produces good quality images that appear to be enhanced at data rates of 1.5 bits/picture element. No large data storage is required, and the computation is small. The quantizer is compared with standard (minimum mean-square error and mean absolute error) one-bit quantizers. Modifications of the basic BTC algorithm are discussed along with the performance of BTC in the presence of channel errors.

I. INTRODUCTION

Since the beginning of the use of digital techniques for image processing, there has been a desire to find ways of coding images efficiently. The number of bits required to preserve high dynamic range and resolution in a typical PCM picture ranges from 10^6 to 10^8 . Many, efficient image coding schemes have evolved [1], popular examples are the Cosine transform of Chen and Smith [2] and predictive coding (DPCM) [3].

In this paper we will present a new technique called Block Truncation Coding (BTC) that has been developed at Purdue University in the past two years [4]–[5]. This technique uses a one bit nonparametric quantizer adaptive over local regions of the image. The quantizer that shows great promise is one that preserves local statistics of the image.¹

Paper approved by the Editor for Data Communication Systems of the IEEE Communications Society for publication after presentation at ICC'78, Toronto, Ont., Canada, June 1978. Manuscript received October 30, 1978; revised March 22, 1979. This work was supported by the Rome Air Development Center, Griffiss AFB-RADC, under Grant F75C0082 covering the period from April 1, 1977 to October 31, 1978.

The authors are with the School of Electrical Engineering, Purdue University, West Lafayette, IN 47907.

¹ At the time of presentation of our ICC paper [5], a method similar to BTC was presented in Japan by Kishimoto *et al.* [6]–[8].

In this paper the BTC algorithm is presented and compared with some common techniques of image compression. Modifications to BTC are presented including some hybrid techniques. The performance of BTC in the presence of channel errors is also discussed.

II. BASIC BTC ALGORITHM

For the study presented here the image will be divided into 4×4 pixel blocks, and the quantizer will have 2 levels. If one uses the classical quantization design of Max [9] which minimizes the mean square error, one must know, *a priori*, the probability density function of the pixels in each block. This same knowledge is also required for the absolute error fidelity criteria of Kassam [10]. Since in general it is not possible to find adequate density function models for typical imagery, we have used nonparametric quantizers for our coding schemes. Nonparametric quantizer design that minimizes either mean square error (denoted MSE) or mean absolute error (denoted MAE) will be presented in Section III. In this section we present the design of a nonparametric quantizer that preserves sample moments (denoted MP); the design of a parametric MP quantizer is presented in [11].

After dividing the picture into $n \times n$ blocks ($n = 4$ for our examples), the blocks are coded individually, each into a two level signal. The levels for each block are chosen such that the first two sample moments are preserved. Let $m = n^2$ and let X_1, X_2, \dots, X_m be the values of the pixels in a block of the original picture.

Then the first and second sample moments and the sample variance are, respectively

$$\begin{aligned}\bar{X} &= \frac{1}{m} \sum_{i=1}^m X_i \\ \bar{X^2} &= \frac{1}{m} \sum_{i=1}^m X_i^2 \\ \bar{\sigma^2} &= \bar{X^2} - \bar{X}^2.\end{aligned}\quad (1)$$

As with the design of any one bit quantizer, we find a threshold, X_{th} , and two output levels, a and b , such that

$$\begin{aligned}\text{if } X_i \geq X_{th} \quad \text{output} &= b \\ \text{if } X_i < X_{th} \quad \text{output} &= a \\ \text{for } i &= 1, 2, \dots, m.\end{aligned}\quad (2)$$

For our first quantizer, we set $X_{th} = \bar{X}$, this reasonable assumption will be modified in Section IV to improve performance. The output levels a and b are found by solving the following equations:

$$\begin{aligned}\text{Let } q &= \text{number of } X_i\text{'s greater than } X_{th}(=\bar{X}) \\ \text{then to preserve } \bar{X} \text{ and } \bar{X^2} \\ m\bar{X} &= (m-q)a + qb\end{aligned}\quad (3)$$

and

$$m\bar{X^2} = (m-q)a^2 + qb^2$$

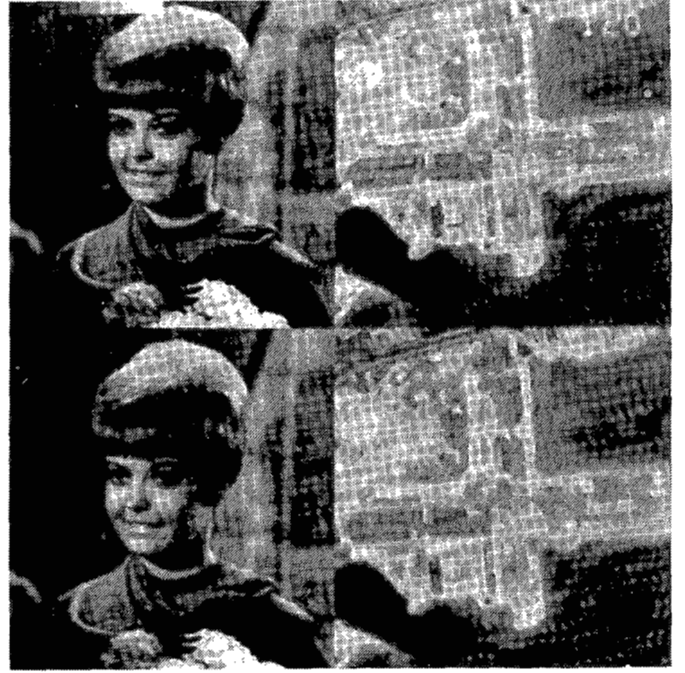


Figure 1. Results using the basic BTC algorithm. The original images (top) are 256×256 pixels with nominal 8 bits gray level resolution. The coded images (bottom) have a data rate of 2 bits/pixel.

Solving for a and b :

$$\begin{aligned}a &= \bar{X} - \bar{\sigma} \sqrt{\frac{q}{m-q}} \\ b &= \bar{X} + \bar{\sigma} \sqrt{\frac{m-q}{q}}.\end{aligned}\quad (4)$$

Each block is then described by the values of \bar{X} , $\bar{\sigma}$ and an $n \times n$ bit plane consisting of 1's and 0's indicating whether pixels are above or below X_{th} . Assigning 8 bits each to \bar{X} and $\bar{\sigma}$ results in a data rate of 2 bits/pixel. The receiver reconstructs the image block by calculating a and b from Equation 4 and assigning these values to pixels in accordance with the code in the bit plane. (An example of coding a 4×4 picture block is presented in the Appendix.)

Examples of this coding system are shown in Figure 1. The block boundaries are not visible in the reconstructed pictures nor is the quantization noise visible in regions of the picture where there is little change in luminance. Here the levels a and b are close together. They are widely spaced only in regions where large changes of luminance occur; but it is well known [13] that large changes of luminance mask noise. Thus BTC encoding makes use of the masking property in human vision. The most noticeable improvement of the reconstructed picture is a little raggedness of sharp edges. In the next section we will present methods for improving the image quality and reducing the bit rate.

Because the calculations are relatively simple and the storage of data small, BTC is fairly easy to implement. A recent study has shown that BTC can be realized on an integrated circuit chip [12].

III. OTHER NONPARAMETRIC QUANTIZER SCHEMES

As mentioned in Section II, other techniques can be used to design a one bit quantizer. Use of rate-distortion theory seems theoretically attractive but somewhat impractical for real images [14]–[15]. In this section we will discuss the use of the minimum mean square error (MSE) and minimum mean absolute error (MAE) fidelity criteria for one-bit nonparametric quantizers.

To use the MSE fidelity criterion, one proceeds by first constructing a histogram of the X_i 's (i.e., sorting the X_i 's). Let Y_1, Y_2, \dots, Y_m be the sorted X_i 's; i.e., $Y_1 \leq Y_2 \leq \dots \leq Y_m$. Again let q be the number of X_i 's greater than X_{th} . Then a and b are found by minimizing

$$J_{MSE} = \sum_{i=1}^{m-q-1} (Y_i - a)^2 + \sum_{i=m-q}^m (Y_i - b)^2 \quad (5)$$

where

$$a = \frac{1}{m-q} \sum_{i=1}^{m-q-1} Y_i$$

$$b = \frac{1}{q} \sum_{i=m-q}^m Y_i.$$

One obvious way to solve this problem is to try every possible threshold (there are at most $m-1$ thresholds) and pick the one with smallest J_{MSE} . Assuming a and b have 8-bit resolution, this gives a data rate of 2 bits/pixel.

The problem of using the MAE fidelity criterion is very similar to the MSE. The values a and b are found by minimizing

$$J_{MAE} = \sum_{i=1}^{m-q-1} |Y_i - a| + \sum_{i=m-q}^m |Y_i - b| \quad (6)$$

where

$$a = \text{median of } (Y_1, Y_2, \dots, Y_{m-q-1})$$

$$b = \text{median of } (Y_{m-q}, \dots, Y_m).$$

Here again the nonparametric quantizer is arrived at by an exhaustive search. Results using these quantizers and BTC are shown in Figures 2 and 3. As mentioned in Section II it is possible to use a parametric quantizer once the probability density function of the pixels is known (or guessed). In Figures 2 and 3 results are presented for a parametric MSE quantizer where the pixels are assumed to be uniformly distributed over each block. Table I has the computed mean square error and mean absolute error measures for each image. As anticipated the MSE quantizer has the smallest computed mean square error measure and the MAE quantizer has the smallest computed mean absolute error measure. The performance of BTC is quite good when compared to these standard fidelity criteria. The advantage of using a nonparametric MP quantizer is that the quantizer formulation is available in *closed form*; this greatly simplifies the computational load.



Figure 2. Results using various fidelity criterion. All data rates are 2.0 bits/pixel. Upper left: minimum mean square error; Upper right: minimum mean absolute error; Lower left: moment preserving; Lower right: minimum mean square error and also assuming image data uniformly distributed each block.

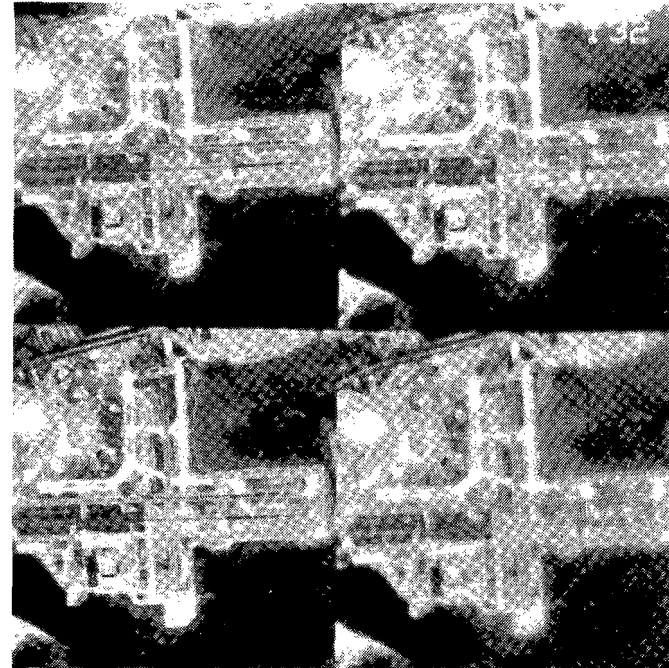


Figure 3. These four pictures were produced as described in Figure 2 using the other original.

IV. BTC MODIFICATIONS

In many image coding schemes it is desired to obtain data rates less than 2 bits/pixel. An obvious way of achieving this is to assign less than 8 bits to \bar{X} and $\bar{\sigma}$. Experimental evidence has indicated that coding \bar{X} with 6 bits and $\bar{\sigma}$ with 4 bits introduces only a few perceivable errors. Now the data rate is 1.63 bits/pixel. Better performance could be obtained by quan-

TABLE I
COMPUTED MEAN SQUARE ERROR AND MEAN ABSOLUTE
ERROR MEASURES FOR VARIOUS QUANTIZATION
SCHEMES

	Mean Square Error	Mean Absolute Error
Data from Figure 2:		
Using MSE quantizer	32.94	3.54
Using MAE quantizer	37.13	3.28
Using BTC	40.89	3.91
Using parametric MSE quantizer and assumed uniform density	44.64	4.23
Data from Figure 3:		
Using MSE quantizer	47.14	4.39
Using MAE quantizer	53.22	4.10
Using BTC	58.34	4.85
Using parametric MSE quantizer and assumed uniform density	64.02	5.42

tizing \bar{X} and $\bar{\sigma}$ jointly, using 10 bits. \bar{X} is assigned most bits in blocks where $\bar{\sigma}$ is small and fewest bits where $\bar{\sigma}$ is large.

Additional savings could be realized by efficiently coding the bit plane. Entropy calculations indicate that 0.85 bits/pixel would be sufficient for the bit plane. Such small improvement does not justify the increased complexity of the system and the increased variability to error that efficient coding entails.

Setting the threshold of the quantizer at \bar{X} , removes a possible degree of freedom for optimizing the encoding. Allowing the threshold to be a variable permits the encoding to preserve not only the first two sample moments but also the third sample moment. To analyze this, we make use of the sorted pixel values Y_i . The third moment can be expressed as

$$\bar{X^3} = \frac{1}{m} \sum_{i=1}^m X_i^3 = \frac{1}{m} \sum_{i=1}^m Y_i^3. \quad (7)$$

The problem then is finding a , b , and q to preserve \bar{X} , $\bar{X^2}$, and $\bar{X^3}$ (q defines the threshold since it specifies the number of X_i 's greater than X_{th}), Equation 3 now becomes

$$\begin{aligned} m\bar{X} &= (m-q)a + qb \\ m\bar{X^2} &= (m-q)a^2 + qb^2 \\ m\bar{X^3} &= (m-q)a^3 + qb^3. \end{aligned} \quad (8)$$

Having the solutions

$$\begin{aligned} a &= \bar{X} - \sigma \sqrt{\frac{q}{m-q}} \\ b &= \bar{X} + \bar{\sigma} \sqrt{\frac{m-q}{q}} \\ q &= \frac{m}{2} \left[1 + A \sqrt{\frac{1}{A^2 + 4}} \right] \end{aligned} \quad (9)$$

where

$$A = \frac{3\bar{X}\bar{X^2} - \bar{X^3}2(\bar{X})^3}{\bar{\sigma}^3}$$

$$\bar{\sigma} \neq 0.$$

If $\bar{\sigma} = 0$, then $a = b = \bar{X}$.

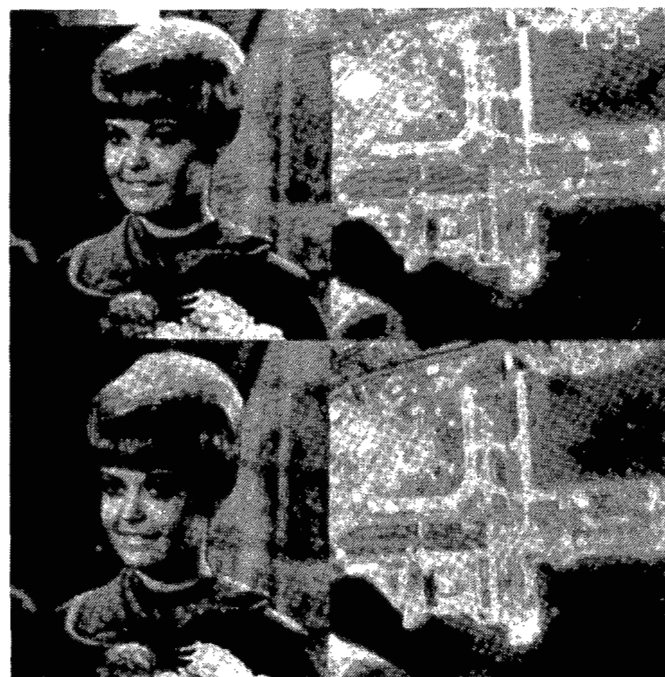


Figure 4. Results of BTC using third moment preserving threshold selection. Original images are at the top. Coded images are at the bottom. Data rate is 2.0 bits/pixel.

In general the value of q obtained will not be an integer, so in practice it must be rounded to the nearest integer. An interesting interpretation of Equation 9 is that the threshold is nominally set to the sample median and biased higher or lower depending upon the value of the third sample moment which is a measure of skewness of the Y_i 's. This threshold selection requires no extra computation at the receiver (decoder), but the transmitter (encoder) does have extra processing. This method of threshold selection is far easier to implement than are the nonparametric quantizers discussed in Section III since they require an exhaustive search.

Figure 4 shows results using this threshold selection. It improves subtle features (such as near edges) of the image that are usually important in analysis of aerial photography imagery. This improvement will be discussed in the following section.

V. PERFORMANCE EVALUATION OF BTC

Recent studies at Purdue University have evaluated various image coding techniques for transmitting aerial reconnaissance images over noisy channels [16]. BTC, transform, Hybrid [17] and one other technique were evaluated by professional photo analysts.

Although BTC did not perform as well as transform coding in the photo interpreters evaluation, it proved superior to the other techniques. In the presence of many channel errors, BTC was superior to all of the other techniques. Some images used in the study are shown in Figures 5-8. In these figures BTC is compared with the Chen and Smith [2] method of transform coding and Hybrid coding. The computed mean square errors and mean absolute errors are shown in Table II. Our study has shown that the mean square error and mean absolute error measure cannot be easily correlated with photo analysts' evaluations. In some cases, images with large mean square errors were evaluated higher than images with smaller mean square errors. It should be noted that BTC requires a significantly smaller computational load and much less memory than

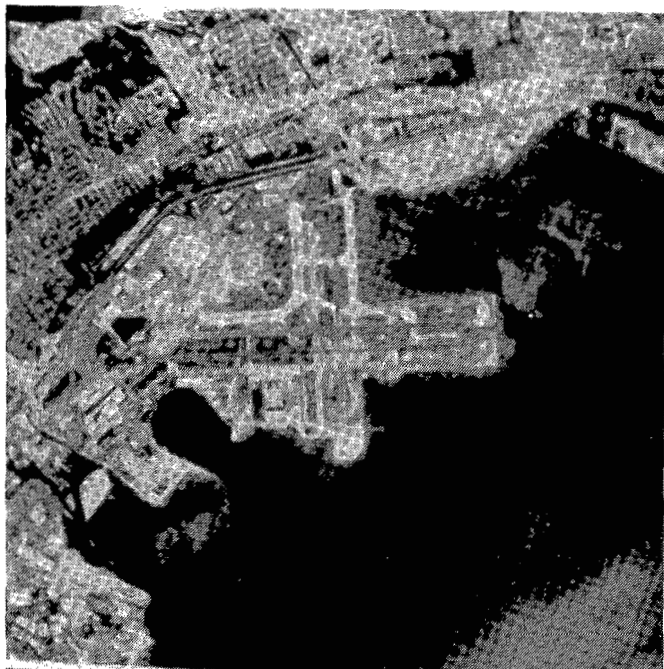


Figure 5. Original image used in comparison study. Image is 512×512 pixels with nominal 8 bits gray level resolution.



Figure 6. Results of coding original (Figure 5) using BTC with third moment preserving threshold selection. Data rate is 1.63 bits/pixel.



Figure 7. Results of coding original (Figure 5) using Chen and Smith [2] method of Cosine Transform coding. Data rate is 1.63 bits/pixel.



Figure 8. Results of coding original (Figure 5) using Hybrid coding [17]. Data rate is 1.63 bits/pixel.

TABLE II
COMPUTED MEAN SQUARE ERROR AND MEAN ABSOLUTE
ERROR MEASURES FOR COMPARISON IMAGES SHOWN IN
FIGURES 6-11 AND FIGURE 13

	Mean Square Error	Mean Absolute Error
Figure 6	84.22	5.94
Figure 7	67.13	6.32
Figure 8	125.84	6.12
Figure 9	115.09	6.29
Figure 10	115.31	7.06
Figure 11	140.33	6.67
Figure 13	74.67	5.72



Figure 9. BTC coding with channel error probability of 10^{-3} . Data rate is 1.63 bits/pixel.



Figure 11. Hybrid coding with channel error probability of 10^{-3} . Data rate is 1.63 bits/pixel.



Figure 10. Chen and Smith coding with channel error probability of 10^{-3} . Data rate is 1.63 bits/pixel.



Figure 12. Enlarged section of image from Figure 6 (left) and Figure 7 (right).

transform or Hybrid coding. For instance, the Chen and Smith method requires the two-dimensional Cosine transform over every 16×16 image block and also requires multiple passes through the transform data to collect various statistics about the transform coefficients. It should also be mentioned that BTC requires no sophisticated error protection as do the other coding methods evaluated. Figures 9-11 show the results of each coding method in the presence of channel errors. The

channel was assumed to be binary symmetric with the probability of a bit error of 10^{-3} .

One of the advantages of BTC is that luminance edges are emphasized. Figure 12 shows an enlarged section of an image coded using the Chen and Smith method and BTC. The edges using the transform coding method are not as sharp as the BTC image.

As with all noninformation preserving image coding, coding artifacts are produced in the image. It became apparent very early in this study that BTC produces artifacts that are very different than transform coding. They are usually seen in regions around edges and in low contrast areas containing a sloping gray level. As mentioned above, BTC does produce sharp edges; however, these edges do have a tendency to be ragged. Transform coding usually produces edges that are blurred and smooth. The second problem in low contrast regions is due to inherent quantization noise in the one bit quantizer. Here sloping gray levels can turn into false contours. Preliminary experiments have indicated that pre- and post-



Figure 13. Results of Hybrid Formulation of BTC. Data rate is 1.88 bits/pixel.

processing of the image can reduce the effects of both these artifacts while simultaneously reducing the mean square error and mean absolute error. It should be emphasized that these coding artifacts are problems in high resolution aerial reconnaissance images where minute objects are important. These coding artifacts usually are not visible in typical "head and shoulders" imagery.

VI. HYBRID FORMULATION OF BTC

BTC uses only first-order information and does not exploit the two-dimensional structure of the image within each block as do most other forms of image coding. For example in two-dimensional transform coding the transform coefficients contain information about variations in the picture in both directions. Also BTC generally has a poor response near the spatial frequency of $1/2$ cycle per block.

One method to overcome this disadvantage is a hybrid formulation. First a highly compressed Cosine transform coded image is subtracted from the original image. For the results presented here the transform picture was obtained by taking the two-dimensional Cosine transform over 16×16 pixel blocks. Only the eight non-dc coefficients in the low frequency section of each block were retained. This corresponds to a zonal filtering method with a bit rate of 0.25 bits/pixel for the highly compressed image. BTC was then used on this difference picture and the recombination formed at the receiver. While this did increase the computational load, the improvement seemed to be significant enough to give this method further attention. Figure 13 presents results of this hybrid method. Table II has the mean square error and mean absolute error measures for Figure 13.

VII. CONCLUSIONS

A new, simple technique has been described with modifications to improve its performance. The resulting recon-

structed image has artifacts quite different from those produced by other techniques, but the resulting images are comparable and in some ways superior to those produced by the most sophisticated techniques available. This method produces a coded image that is more robust in the presence of channel errors and requires very little error protection overhead.

ACKNOWLEDGMENT

The authors would like to thank Dr. John Gamble of the Rome Air Development Center for his helpful criticism of this work. We would also like to thank Richard P. Petroski and his colleagues of the Rome Research Corporation who provided the expert photo evaluations mentioned in Section V.

The authors would also like to thank Professor Steven Bass of Purdue for suggesting the hybrid formulation of BTC and Ali Tabatabai and Paul Stiling also of Purdue for providing the transform and Hybrid coded images.

APPENDIX

To illustrate coding a 4×4 picture block using Block Truncation Coding, let us quickly review the basic BTC algorithm:

- a) the image is divided in small nonoverlapping blocks such as 4×4 .
- b) The first and second sample moments are computed.
- c) A bit plane is constructed such that each pixel location is coded as a "one" or a "zero" depending on whether that pixel is greater than \bar{X} .
- d) The bit plane, \bar{X} , and $\bar{\sigma}$ are sent to the receiver.
- e) The picture block is reconstructed such that \bar{X} and $\bar{\sigma}$ (alternatively \bar{X}^2) are preserved. That is, pixels in the bit plane that are "0" are set to "a" and the "1"s are set to "b" in Equation 4. For example, suppose a 4×4 picture block is given by the following:

$$X_{ij} = \begin{bmatrix} 121 & 114 & 56 & 47 \\ 37 & 200 & 247 & 255 \\ 16 & 0 & 12 & 169 \\ 43 & 5 & 7 & 251 \end{bmatrix}$$

so

$$\bar{X} = 98.75$$

$$\bar{\sigma} = 92.95$$

$$q = 7$$

and

$$a = 16.7 \cong 17$$

$$b = 204.2 \cong 204$$

the bit plane is

$$\begin{bmatrix} 1 & 1 & 0 & 0 \\ 0 & 1 & 1 & 1 \\ 0 & 0 & 0 & 1 \\ 0 & 0 & 0 & 1 \end{bmatrix}$$

The reconstructed block becomes

$$\begin{bmatrix} 204 & 204 & 17 & 17 \\ 17 & 204 & 204 & 204 \\ 17 & 17 & 17 & 204 \\ 17 & 17 & 17 & 204 \end{bmatrix}$$

and the sample mean and variance are preserved.

REFERENCES

- [1] A. Habibi, "Survey of Adaptive Image Coding Techniques," *IEEE Trans. on Communications*, Vol. COM-25, No. 11, pp. 1275-1284, Nov. 1977.
- [2] W-H. Chen and C. H. Smith, "Adaptive Coding of Monochrome and Color Images," *IEEE Trans. on Communications*, Vol. COM-25, pp. 1285-1292, Nov. 1977.
- [3] J. B. O'Neal, "Predictive Quantizing System (DPCM) for the Transmission of Television Signals," *BSTJ*, Vol. 45, pp. 689-721, May-June 1966.
- [4] O. R. Mitchell and E. J. Delp, "Image Compression Using Block Truncation," Purdue University-Purdue Research Foundation, Record and Disclosure of Invention, dated April 8, 1977. This document is available from the authors.
- [5] O. R. Mitchell, E. J. Delp, and S. G. Carlton, "Block Truncation Coding: A New Approach to Image Compression," *Conference Record, 1978 IEEE International Conference on Communications (ICC'78)*, Vol. I, June 4-7, 1978, pp. 12B.1.1-12B.1.4.
- [6] T. Kishimoto, E. Mitsuya, and K. Hoshida, "A Method of Still Picture Coding by Using Statistic Properties," (in Japanese) National Conference of the Institute of Electronics and Communications Engineers of Japan, March 1978, No. 974.
- [7] T. Kishimoto, E. Mitsuya, and K. Hoshida, "An Experiment of Still Picture Coding by Block Processing" (in Japanese) National Conference of the Institute of Electronics and Communications Engineers of Japan, March 1978, No. 975.
- [8] T. Kishimoto, E. Mitsuya, and K. Hoshida, "Block Coding of Still Pictures," (in Japanese), Technical Group of Communication System of the Institute of Electronics and Communication Engineers of Japan, pp. 63-69, July 1978.
- [9] J. Max, "Quantizing for Minimum Distortion," *IRE Trans. on Info. Theory*, Vol. IT-6, pp. 7-12, March 1960.
- [10] S. A. Kassam, "Quantization Based on the Mean-Absolute-Error Criterion," *IEEE Trans. on Communications*, Vol. COM-26, pp. 267-270, Feb. 1978.
- [11] E. J. Delp and O. R. Mitchell, "Some Aspects of Moment Preserving Quantizers," in *Conf. Rec., 1979 IEEE International Conference on Communications*, (ICC'79), vol. I, June 10-14, pp. 7.2.1-7.2.5.
- [12] W. L. Eversole, D. J. Mayer, F. B. Frazee, an T. F. Cheek, "Investigation of VLSI Technologies for Image Processing," *Proceedings: Image Understanding Workshop*, Pittsburgh, PA, Nov. 14-15, 1978. Sponsored by the Defense Advanced Research Projects Agency (DARPA), pp. 191-195. (Copies available from the Defense Documentation Center (DDC) under Accession No. ADA 052903).
- [13] D. Jameson and L. M. Hurvich (editors), *Handbook of Sensory Physiology: Visual Psychophysics*, New York; Springer-Verlag, 1972.
- [14] T. Berger, *Rate Distortion Theory*, Englewood Cliffs: Prentice-Hall, 1971.
- [15] J. L. Munnos and D. J. Sakrison, "The Effects of a Visual Fidelity Criterion on the Encoding of Images," *IEEE Trans. on Information Theory*, Vol. IT-20, pp. 525-536, July 1974.
- [16] O. R. Mitchell, S. C. Bass, E. J. Delp, and T. W. Goeddel, "Coding of Aerial Reconnaissance Images for Transmission over Noisy Channels," issued as Rome Air Development Center (RADC) Technical Report, Griffiss Air Force Base, NY. Report No. RADC-TR-78-210. (This report is available from the National Technical Information Service, Accession No. ADA 061539).
- [17] A. Habibi, "Hybrid Coding of Pictorial Data," *IEEE Trans. Commun.*, Vol. COM-22, pp. 614-624, May 1974.

Effects of Digital Demodulation on Component Coding of NTSC Color Signals

ERIC DUBOIS

Abstract—Effects of nonideal filtering in the digital demodulation of the composite NTSC signal into luminance and chrominance components on the coding of the luminance component are discussed. The residual chrominance component is shown to cause degradation in prediction and/or motion detection algorithms which are based on line or frame difference signals. Simple techniques for reducing these effects using chrominance-band rejection filters are presented and the efficacy of these methods are verified by simulation.

I. INTRODUCTION

A common technique for coding NTSC color signals for bandwidth compression is component coding, whereby the composite NTSC signal is separated into luminance and chrominance components, and each is coded individually. There are several advantages to performing this demodulation using digital filtering techniques [1]. Analog demodulators require the use of high precision analog delay lines which may require frequent alignment, while, of course, digital filters require no such alignment. Also, in all-digital installations, the use of analog filters would require additional D/A and A/D conversion. However, due to the high data rates associated with color video signals, only relatively low order filters are currently cost effective. Digital demodulation using such filters has not been widely used in color codecs, partly due to the residual chrominance effects which will be described in this paper.

The frequency of the color subcarrier in an NTSC signal is such that it changes in phase by 180° from line to line and from frame to frame. When the composite NTSC signal is separated into luminance and chrominance components by digital filtering, a residual chrominance component remains in the luminance component due to nonideal filtering. Taking a frame difference or line difference of this luminance signal causes the residual chrominance component to be reinforced due to the 180° phase shift of the subcarrier, while the luminance component cancels to a large extent, due to line-to-line or frame-to-frame correlation. This results in a substantial spurious component in the difference signal, located in the chrominance band, causing degradation in the performance of prediction and/or motion detection algorithms based on line or frame differences. These effects can be minimized by passing the difference signal through a chrominance-band rejection filter, similar to that used to separate the luminance from the composite waveform. This paper examines the application of this principle to a number of schemes for coding the luminance component of the NTSC signal.

Paper approved by the Editor for Data Communication Systems of the IEEE Communications Society for publication after presentation at the 9th Biennial Symposium on Communications, Queen's University, Kingston, Ont., Canada, August 1978. Manuscript received September 8, 1978; revised April 2, 1979. This work was supported in part by the National Research Council of Canada under Grant A0022.

The author is with INRS-Telecommunications, University of Quebec, Verdun, P.Q., Canada H3E 1H6.